Hydrometeor Classification at MeteoSwiss

Jordi Figueras i Ventura, Marco Boscacci, Marco Gabella and Urs Germann

MeteoSwiss, Via ai Monti 146, 6605 Locarno, Switzerland
(Dated: 18 July 2014)

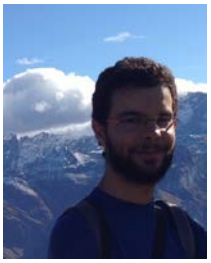

Jordi Figueras

1 Introduction

MeteoSwiss is in the process of deploying the 4th generation of its operational weather radar network. The network consists in a total of 5 identical C-band Doppler-polarimetric weather radars. At the moment 4 radars are operational on Albis, La Dôle, Monte Lema, and Pointe de la Plaine Morte. A 5th radar is under construction on Weissfluhjoch and it is expected to be operational by 2016. Germann et al (2014) provide more details on the design of the network.

In the new generation, polarimetry is extensively used in the data processing. Already implemented are data quality monitoring tools, a clutter identification algorithm and basic processing to estimate the differential phase ϕ_{dp} and the specific differential phase K_{dp} and correct the reflectivity Z_h and differential reflectivity Z_{dr} for precipitation-induced attenuation (Figueras i Ventura et al, 2013). K_{dp} is already used to estimate heavy rainfall.

Currently under development is an hydrometeor classification algorithm based on polarimetric variables and model data. Multiple classification schemes based on polarimetry are described in the literature. (See for example Liu and Chandrasekar (2000), Dolan and Rutledge (2009), Park et al. (2009), Marzano et al. (2010), Al-Sakka et al. (2013), etc.). They approach differ in many aspects: the number and definition of possible hydrometeor types, the frequency band of applicability (S, C or X), the type of classification technique (fuzzy logic, neural network, Bayes, etc.), the method to construct the membership functions (observation based versus model based), etc. Some of them have been applied successfully on an operational or semi-operational basis. The mere existence of such a large variety of classification schemes is an indicator that polarimetric hydrometeor classification is not yet mature and that much research is needed to optimize it.

At MeteoSwiss it was decided to develop a classification scheme adapted to the specificities of both the radar network design and the orographic and climatologic conditions. The main goals of the classification scheme are two-fold: in the first place, to improve the quantitative precipitation estimation QPE by properly identifying the different hydrometeors and therefore being able to fine tune the relations between polarimetric variables and equivalent rainfall rate; secondly, to detect potentially hazardous meteorological phenomena such as hail or snow. Care has been placed in designing a software flexible so that new developments in the definition of the type of hydrometeors, the use of new types of input data, the estimation of the uncertainty of the data or the modelling of the scattering properties of each hydrometeor can be easily incorporated.

2 Design philosophy

The classification scheme is based on fuzzy logic. This decision is driven by the fact that is a computationally fast algorithm and that the construction of the membership functions (MF) can be either based on data analysis, based on heuristic knowledge or a combination of both. In our case, MF are based on the modelling of the scattering properties of individual hydrometeor types rather than on expert identification of radar observations. Such approach is favored for two reasons: In the first place, it avoids possible biases due to radar miss-calibration, attenuation, partial beam blocking, noise, misclassification, etc. Secondly, having a complete control of the microphysical model underlying the classification it allows the generation of MF at different elevations, frequency bands, etc. Moreover, the same modeling provides information on the relationship between polarimetric variables and bulk-microphysics such as the equivalent liquid water content LWC or equivalent rainfall rate that can be used in the estimation of precipitation, or of phenomena contributing to the uncertainty in the measurements such as attenuation or the value of the backscatter co-polar differential phase δ_{co}. Obviously the drawback of such approach is the risk of having unrealistic (due to the lack of data) or oversimplified microphysical models that are not representative of the observations.

The classification is performed on a gate-by-gate basis. Since the volumetric scan consists in 20 different elevations ranging from -0.2° to 40°, 20 different sets of membership functions are computed. The main output of the classification is the dominant type of hydrometeor and the probability given by the fuzzy logic algorithm. Additionally the second most probable hydrometeor and its probability is also provided. The difference in the probability between the first and the second output can be interpreted as a measure of confidence in the classification. Moreover, this can also be used in the clustering of the data.

The input data consists in the polarimetric variables (Z_h, Z_{dr}, K_{dp} and co-polar correlation coefficient ρ_{hv}) and model data from the COSMO-2 numerical weather prediction model. Clutter in the polarimetric data is filtered a-priori. Estimated biases are corrected as well. A basic attenuation correction is also applied. The COSMO-2 data has a resolution of 2.2 km^2 with 60

different altitude levels with heterogeneous spacing (more levels close to ground level). There are new runs every 3 h available within 1 h after the run and with a temporal resolution of 1 h. The COSMO-2 data is interpolated both in time and space using the nearest neighbor so that a value is assigned to each range gate. At the moment the only data used is temperature because it is considered the most discriminating variable and its reliability is sufficiently high.

The MF of the polarimetric variables are two-dimensional (Z_h-Z_{dr}, Z_h- K_{dp} and Z_h-ρ_{hv}). The basic shape of the polarimetric MF is driven by the results of the modelling of each hydrometeor. The scattering properties of each hydrometeor are simulated assuming various temperatures and particle size distribution (PSD). For each reflectivity level, the minimum and the maximum of the polarimetric variable obtained in the simulations are considered the MF limits. The fuzziness of the MF is introduced by computing the uncertainty of the polarimetric variables in real time. At the moment the uncertainty considered is that caused by the natural fluctuation due to the limit number of independent samples used in the computation of the polarimetric variables (Kostinski, 1994, Bringi and Chandrasekar 2001). If properly characterized, other sources of uncertainty such as the error committed in the correction of precipitation-induced attenuation may be added as well. The model variables have a 1-dimensional MF with a trapezoidal shape.

The probability of an hydrometeor i is computed using the following formula:

$$A_i = \frac{\sum_{\forall j} w_j P^{(i)}(V_j)}{\sum_{\forall j} w_j} P^{(i)}(T)$$

Here $P^{(i)}(V_j)$ is the membership function of each polarimetric variable, $P^{(i)}(T)$ is the membership function of the temperature and w represents the weights applied to each polarimetric variable according to their confidence index. Currently considered weights are the level of partial beam blockage PBB, attenuation (derived from ϕ_{dp}), ρ_{hv} and signal to noise ratio SNR.

The following hydrometeor types are considered: rain, ice crystals, aggregates (dry snow), melting snow, graupel/melting graupel and hail/melting hail. Additionally there is a general class precipitation which is applied when the probability of all the other classes is below a certain threshold. It should be noticed that by hydrometeor type what is considered is the dominant hydrometeor. MeteoSwiss radars cover a range of up to 240 km and at such large distances, where the radar beam is broaden, a mix of hydrometeors is likely. At such distances it may not be possible to assign a particular hydrometeor type as dominant. Therefore the existence of a general class precipitation is fully justified. The non-distinction between hail and melting hail is due to the fact that below the melting layer hail suffers always some degree of melting and therefore completely dry hail is rarely observed. Graupel during the warm period undergoes similar processes. In winter though graupel may be formed when melting snow refreezes due to a thermal inversion close to ground. In such case it may exist in a completely solid form on the ground.

3 Hydrometeor modelling

The hydrometeor modelling is a two-step process. In the first step the scattering properties of each individual size particle is computed using the T-matrix method. In the second, the polarimetric variables of an ensemble of hydrometeors characterized by their PSD are calculated. In order to characterize as reliably as possible the polarimetric properties of each hydrometeor species, the process is repeated for each hydrometeor for different PSD, temperatures, densities, etc. To this aim, a software package has been developed within MeteoSwiss. The software computes not only the polarimetric variables used in the classification (Z_h, Z_{dr}, ρ_{hv}, and K_{dp}) but also other intrinsic scattering properties such as horizontal attenuation A_h, differential attenuation A_{diff}, backscatter co-polar differential phase δ_{co} or linear depolarization ratio LDR. Additionally, it also computes bulk microphysical parameters such as LWC and rainfall rate. The IDL language is used for the input and output management and the computation of the polarimetric variables. The actual computation of the scattering properties of each hydrometeor is performed using the code from Mischenko (2000) for homogeneous hydrometeors or the method followed by Depue et al. (2007) in the case of hydrometeors best represented as having an inner core and an outer shell with different characteristics.

Because each hydrometeor type has differing particularities, each one has its own dedicated software. Generally speaking the input parameters for the computation of individual hydrometeors are temperature and size. The dielectric constant of pure ice or water in the hydrometeor is computed as a function of temperature using the relations from Matzler (2006). In the case of solid or mixed phase hydrometeors, density is also specified since it is used in the computation of the dielectric constant of the mixture of air, ice and (eventually) water. For mixed phase hydrometeors such as melting snow, hail or graupel the initial density is modified according to the degree of melting.

The hydrometeors are represented as oblate particles. In the case of rain, the axis ratio is computed as a function of size using the same parameterization as Thurai et al. (2007). For ice crystals, snow, hail and graupel the initial axis ratio is user-defined. For melting hydrometeors there is a smooth transition between the axis ratio of the initial dry hydrometeor and that of a completely melted one as a function of mass water fraction. The relations are similar to those of Ryzhkov et al. (2011).

Solid hydrometeors and rain are computed using the single layer code by Mischenko (2000). Mixed phase hydrometeors are more complex to model. Hail and graupel, which has high density ice, is modelled as having an inner core of ice

surrounded by an outer core of water. Once the core is soaked a water layer forms at the surface. Aggregates are modelled as a two-layer hydrometeor with a denser ice core surrounded by a less dense shell. When melting, the outer layer melts faster and therefore the relative position of the transition between the inner core and the outer layer is modified (Fabry and Szyrmer, 1999).

Generally speaking, a gamma or exponential PSD is assumed for each hydrometeor type with exact relations derived from literature. Drop size distribution from rain can as well be input directly from disdrometer measurements. For each hydrometeor type the equivalent liquid water content and equivalent rainfall rate are also computed. Relations between hydrometeor type and size and terminal velocity are also obtained from literature. The orientation angle of the particle is user defined. The azimuthal orientation of the particle is considered uniformly distributed while the polar orientation (canting angle) is considered Gaussian of mean 0° and standard deviation variable according to hydrometeor type.

The outputs of the program are the polarimetric variables, rainfall rate and liquid water content as a function of dsd for a specific hydrometeor type set in specific conditions of temperature, standard deviation of the canting angle, hydrometeor density, etc. The output is written in a binary format. Plots relating the polarimetric variables in the .gif format are also computed. Another software set groups the output results for a specific hydrometeor type computes the minimum and maximum value of Z_{dr}, ρ_{hv} and K_{dp} at each reflectivity level and derive from them the membership function.

4 Preliminary results

Figure 1 summarizes the results of the simulations of the various hydrometeors. The simulations were performed at different elevations and for different temperatures and assumptions on the particle size distribution. As it can be observed, there is a large overlapping between the MF of the different hydrometeors, hence the need to use additional information such as temperature in order to improve the classification.

In our simulations of ice crystals (dark green in Figure 1) we have tried to emulate the different crystal habits present in a cloud. Thus, at -30°C we have characterized the crystals as small (<0.3 mm diameter) ice particles with density close to that of pure ice with a shape that can be approximated by an sphere. The PSD is assumed to be exponential with a high number concentration and it is rather narrow. As a result this crystal habit is characterized by weak reflectivity, low Z_{dr} and K_{dp} and high ρ_{hv}. At -20°C we have assumed the crystals to be mostly small plates (up to 1 mm larger dimension) with high density. The shape is approximated by an oblate with small axis ratio. The PSD is assumed broader but with lower number concentration. The results show that this crystal habit is characterized by small Z_h, large Z_{dr}, moderate K_{dp} and somewhat lower ρ_{hv}. -15°C is the habit where most dendrites are generated. We have characterized them as being potentially larger (up to 3 mm larger dimension) with lower density and with the smallest axis ratio (down to 0.15). The results show that they are characterized by moderate Z_h, large K_{dp} and large Z_{dr}. Interestingly, even though dendrites have a smaller axis ratio they exhibit a smaller Z_{dr} than plates due to their lower density. From the figure it is evident that a better characterization of ice crystals is necessary since assuming a single crystal type per habit is not realistic.

Below -15°C we have considered that dry snow (aggregates) (purple in Figure 1) are dominant. They have been characterized as almost spherical particles with density decreasing with size. Snowflakes can be rather large and therefore we have set the maximum size to be 20 mm. The results show that aggregates are characterized by low to moderate reflectivity, low Z_{dr} and K_{dp} values and high ρ_{hv}. When precipitating snowflakes cross the iso-0°C altitude they starts melting and their characteristics (shape, density) undergo a gradual transition from those of solid particles to those of rain. The melting rate is highly dependent on the size and density of the hydrometeor. Our results (Blue in Figure 1) show that melting snow is characterized by moderate to large values of Z_h, a sharp increase in K_{dp}, a moderate increase in Zdr and lower values of ρ_{hv}. This results are coherent with studies of the melting layer although even lower ρ_{hv} values should be expected. We attribute that to the difficulty of simulating the surface irregularities of the flake.

Graupel (orange in Figure 1) is almost spherical in shape like aggregates but with a higher density due to the accumulation of frozen drops. Graupel particles tend to be small (up to 5 mm). Our graupel category accounts for two physically different phenomena: refreezing of snow due to inversion or moderate rimming of ice crystals due to weak upflow. In the 2nd case they start melting as they precipitate so graupel may exist as purely solid or as mixed phase precipitation. When on a mixed phase state the characteristics of graupel (shape, density) undergo a gradual transition from those of solid particles to those of rain. We have not attempted to differentiate the two states in our membership functions. We have simulated the melting graupel as having a coat of water that surrounds an ice nucleus. Excessive water in the coat is shed and accounted as newly formed droplets (Ryzhkov et al. 2013) It can be observed that graupel have similar characteristics than melting snowflakes although with higher Z_{dr} and lower ρ_{hv}, likely due to the larger density of graupel and the change of melting rates with size.

We have simulated hail (light green in Figure 1) in a similar manner as graupel although with larger initial size (up to 40 mm). It can be seen that hail is characterized by very large reflectivity and a large range of values of ρ_{hv}, Z_{dr}, and K_{dp} depending on the degree of melting of the hailstones.

In our simulations of rain (black in Figure 1) we have used DSDs as obtained directly from 2 years of measurements from a high density network of disdrometers (16 disdrometer within 1 km^2) (see Jaffrain and Berne for details on the network) without any a-priori assumption on the shape of the DSD (gamma, exponential). We have simply reduced the dataset to only

rain cases and computed the radar observed DSD as the average of all the disdrometers. We have simulated rain for temperatures ranging from 3 to 30 °C. It can be seen that rain has values ranging from weak to large reflectivity with increasing K_{dp} and Z_{dr} and decreasing ρ_{hv}. The range of values for K_{dp}, Z_{dr} and ρ_{hv} increases significantly with temperature.

Qualitatively our results can be considered realistic and in line with those reported in the literature with the exception of the ρ_{hv} of melting hydrometeors, where the irregularities of the surface are not well captured. It should be noticed the large overlap existing between melting hydrometeors and heavy rain which may rend difficult a proper discrimination. A spatially depending technique such as clustering or algorithms detecting the melting layer available in literature (Giangrande et al. 2008 for example) may be necessary to improve the classification. Finally, the difference between the top and bottom panels in Figure 1 justify the need to obtain a membership function for each elevation. Although at higher elevations there is indeed useful polarimetric information the range of values is much different from those at low elevations.

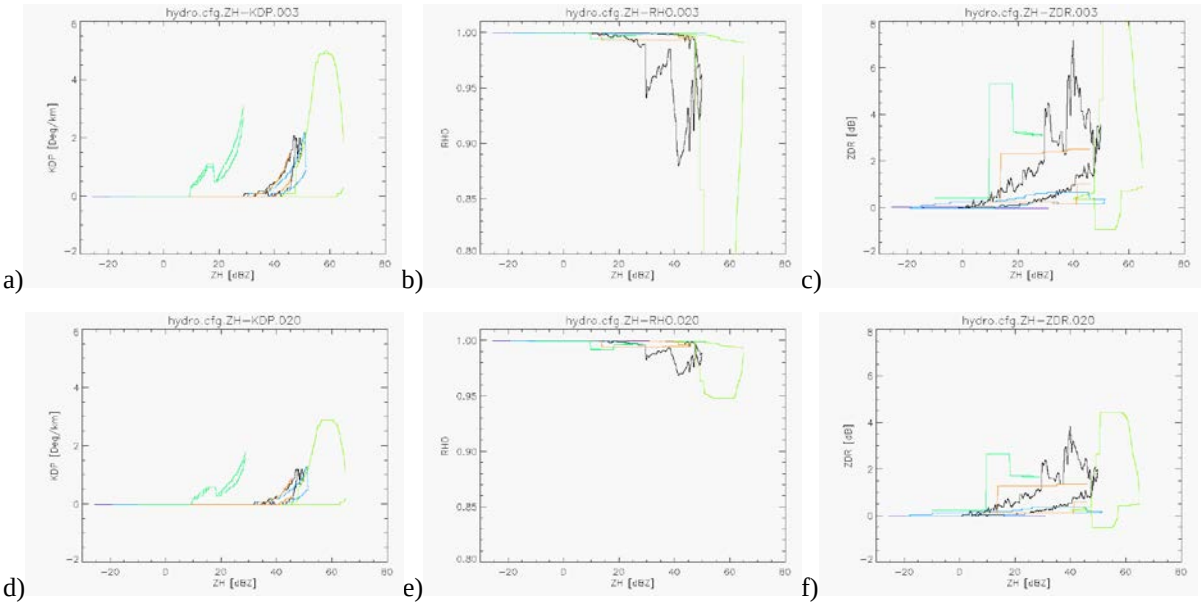

Figure 1: Two dimensional membership functions for elevation 3 (1°, top) and 20 (40°, bottom) of the MeteoSwiss volumetric scan: a) and d) Z_h- K_{dp}, b) and e) Z_h-phv, c) and f) Zh-Zdr.Color code from black, bluish, green, orange: rain, snow, melting snow, ice crystals, hail/melting hail and graupel/melting graupel.

5 Conclusion

An hydrometeor classification algorithm is being developed at MeteoSwiss. The classification scheme is based on fuzzy logic with membership functions derived by modelling the scattering properties of individual hydrometeor types. The modelling software also provides a useful tool for characterizing the relationship between polarimetric variables and bulk micro-physics such as equivalent liquid water content and equivalent rainfall rate.

The preliminary results seem reasonable although much more effort has to be placed in the validation of the membership function and the algorithm. It should be emphasized that the algorithm retrieves the hydrometeor type at range gate level. No attempt has been done to extrapolate it to ground level. Future work includes the construction of a 3-D composite and the exploitation of the information on hydrometeor type to improve the quantitative precipitation estimation.

Acknowledgement

We thank prof. Ryzhkov for providing us with the double layer scattering code.

References

Al-Sakka H. and Boumahmoud, A-A. and Fradon, B. and Frasier, S J. and Tabary, P A New Fuzzy Logic Hydrometeor Classification Scheme Applied to the French X-, C-, and S-Band Polarimetric Radars. // J. Appl. Meteor. Climatol. – 2013. – Vol. 52. – pp. 2328-2344.

Bringi V N. and Chandrasekar, V Polarimetric Weather Radar: Principles and Applications. // 1st ed. Cambridge University Press: 2001.

Depue T K. and Kennedy, P C. and Rutledge, S A Performance of the hail differential reflectivity (HDR) polarimetric radar hail indicator // J. Appl. Meteor. Climatol. – 2007. – Vol. 46. – pp. 1290–1301.

Dolan B. and Rutledge, **S A** A Theory-Based Hydrometeor Identification Algorithm for X-Band Polarimetric Radars. // J. Atmos. Oceanic Technol. – 2009. – Vol. 26. – pp. 2071-2088.

Fabry F. and Szyrmer, **W** Modelling of the Melting Layer. Part II: Electromagnetic. // J. Atmos. Sci. – 1999. – Vol. 56. – pp. 3593-3600.

Figueras i Ventura J. and Boscacci, M. and Clementi, L. and Sideris, I. and Gabella, M. and Germann U Rad4Alp, the new Swiss Doppler polarimetric weather radar network: data quality and first results. // 36th Conference on Radar Meteorology - Breckenridge, CO, 16-20 September 2013.

Germann U. and Boscacci, M. and Clementi, L. and Figueras i Ventura, J. and Gabella, M. and Hering, A. and Sartori, M. and Sideris, I Design and first results of the new fourth generation Swiss radar network. // European Radar Conference ERAD 2014 - Garmisch-Partenkirchen, Germany, 1-5 September 2014.

Giangrande S E. and Krause, J M, and Ryhkov, A V Automatic Designation of the Melting Layer with a Polarimetric Prototype of the WSR-88D Radar. // J. Appl. Meteor. Climatol. – 2008. – Vol. 47. – pp. 1354-1364.

Jaffrain J. and Berne, A Experimental Quantification of the Sampling Uncertainty Associated with Measurements from PARSIVEL Disdrometers. // J. Hydrometeor. – 2011.- Vol. 12. – pp. 780-785.

Kostinski A B Fluctuations of Differential Phase and Radar Measurements of Precipitation. // J. Appl. Meteor. – 1994. – Vol. 33. – pp. 1176-1181.

Liu H. and Chandrasekar, V Classification of Hydrometeors Based on Polarimetric Radar Measurements: Development of Fuzzy Logic and Neuro-Fuzzy Systems, and In Situ Verification. // J. Atmos. Ocean Techn. - 2000. – Vol. 17. – pp. 140-164.

Marzano F S. and Botta, G. and Montopoli, M Iterative Bayesian Retrieval of Hydrometeor Content from X-Band Polarimetric Weather Radar. // IEEE Trans. Geosci. Remote Sens. – 2010. – Vol. 48. – pp. 3059-3074.

Matzler C Thermal Microwave Radiation: Applications for Remote Sensing. // The Institution of Engineering and Technology: 2006.

Mischenko M I Calculation of the amplitude matrix for a nonspherical particle in a fixed orientation. // Appl. Opt. – 2000. – Vol. 39. - pp. 1026-1031.

Park H S. and Ryzhkov, A V. and Zrnić, D S. and Kim, K-E The Hydrometeor Classification Algorithm for the Polarimetric WSR-88D: Description and Application to an MCS. // Wea. Forecasting. – 2009. – Vol. 24. – pp. 730-748.

Ryzhkov A V. and Pinsky, M. and Pokrovsky, A. and Khain, A Polarimetric Radar Observations Operator for a Cloud Model with Spectral Microphysics. // J. Appl. Meteor. Climatol. – 2011. – Vol. 50. - pp. 873-894.

Ryzhkov A V. and Kumjian, M. R., and Ganson, S. M. and Khain, A Polarimetric Radar Characteristics of Melting Hail. Part I: Theoretical simulations Using Spectral Microphysical Modeling. // J. Appl. Meteor. Climatol. – 2013. – Vol. 52. - pp. 2849-2870.

Thurai M. and Huang, G J. and Bringi, V N. and Randeu, W L. and Schönhuber, M Drop Shapes, Model Comparisons, and Calculations of Polarimetric Radar Parameters in Rain. // J. Atmos. Oceanic Technol. - 2007. - Vol. 24. – pp. 1019-1032.